

Submerged Membrane Breakwaters I: A Rahmen Type System Composed of Horizontal and Vertical Membranes

SUNG-TAE KEE*

*Civil Engineering Dept, Seoul National University of Technology, Seoul, Korea
(Received 19 June 2002, accepted 2 September 2002)

ABSTRACT: In the present paper, the hydrodynamic properties of a Rahmen-type, flexible, porous breakwater interacting with obliquely or normal-incident small amplitude waves are numerically investigated. This system is composed of dual vertical porous membranes, hinged at the side edges of a submerged horizontal membrane. The dual vertical membranes are extended downward and hinged at seabed. The effects of permeability, Rahmen-type membrane breakwater geometry, pre-tensions on membranes, relative dimensionless wave number, and incident wave headings are thoroughly examined.

KEY WORDS: Flexible Prous-Membrane, Wave-Flexible Structure Interaction, Oblique Waves, Boundary Element Method

1. Introduction

The flexible and porous structures can be used as a breakwater to effectively reduce both the transmitted and reflected wave heights. The two-dimensional problem of wave interaction with porous flexible structure is of growing importance, and significant studies, in this area, have been conducted by several authors.

The problem of the reflection and transmission of small amplitude waves by a flexible, porous, and thin beam-like breakwater has been explored by Wang and Ren (1993a). Wang and Ren (1993b) have also studied the wave-trapping effect that results from a flexible porous breakwater located in front of a vertical impermeable wall. Yu and Chang (1994) investigated the interaction of surface waves with a submerged, horizontal, porous plate. Cho and Kim (2000) studied the interaction of monochromatic incident waves with a horizontal, porous, flexible membrane in the context of two-dimensional linear hydro-elastic theory, and found that using a proper porous material can further enhance the overall performance of the horizontal, flexible membrane.

The interaction of the monochromatic incident wave with the dual pre-tensioned, inextensible, vertical nonporous-membrane wave barrier, extending the entire water depth, has been investigated by Edmond (1998), using eigenfunction expansions for the velocity potential and linear membrane theory. Cho et al. (1998) developed an analytic solution for

a dual nonporous-membrane system and a boundary integral method solution for more practical dual buoy/membrane wave barriers, with either a surface piercing or fully submerged system in oblique seas.

In the present paper, the hydrodynamic properties of a Rahmen-type porous membrane, interacting with obliquely incident small amplitude waves are numerically investigated. This system is composed of one submerged horizontal porous flexible membrane and two vertical porous membranes, hinged at the both side edges of the horizontal membrane. The two vertical membranes, hinged at the edges of the horizontal membranes, are extended downward, and are hinged at the seabed. The fully submerged Rahmen-type breakwater is introduced, herein, taking into account the marine scenario, water circulation, surface vessel passing, and the reduced hydrodynamic pressures on the body of the structures.

To assess the efficiency of this Rahmen-type porous membrane system, two-dimensional hydro-elastic formulation for two fluid domains was carried out, in the context of linear wave-body interaction theory and Darcy's law. The fluid region is split into two regions: region (1) wave ward, over and in the lee of the structure, and region (2) inside of the structure. It is assumed, for simplicity, that the pre-tensioned membrane is thin, un-stretchable, and free to move only in the transverse direction for vertical membranes, and in the longitudinal direction for the horizontal membrane. The pre-tension is assumed to be externally provided, and is much greater

The first author : Sung-Tae Kee

Email : stkee@snut.ac.kr

than the dynamic tension. The membrane dynamics is modeled, such that there is a tensioned string of zero bending rigidity. The velocity potentials of wave motion are fully coupled with deformations of membranes, taking into account the porosity, based on Darcy's law.

The numerical model is validated in comparison to previously published, numerical studies by Cho and Kim (2000), which are based on eigenfunction expansion of the limiting cases of the horizontal porous membrane in monochromatic waves. The relevant numerical results, presented here, relate to the reflection and transmission coefficients. The corresponding wave forces and the motions of membranes are also investigated, but not presented here. The effects of permeability, Rahmen-type membrane breakwater geometry, pre-tensions on membranes, relative dimensionless wave number, and incident wave headings are thoroughly examined.

Results presented, herein, confirm that the overall performance of the Rahmen-type flexible membranes can be further enhanced by using a proper porous material, since the inclusion of permeability on the membrane eliminates the resonance that aggravates the breakwater performance. The performance of this type of breakwater is found to be highly promising for a wide range of frequency and wave headings if, using Rahmen's geometry, pre-tensions, and permeability, it is properly tuned to the coming waves.

2. Theory and Numerical Method

2.1 Governing Equations

The breakwater system with arbitrary porous and flexible boundaries is composed of a horizontal membrane with a width of W and submerged downward a distance D below the still water level and two vertical membranes extended to the sea bottom, as shown in Fig. 1. A Cartesian coordinate system (x, y) is defined with x measuring in the direction of wave propagation from a point mid-way between the vertical membranes, and y measuring upward from the still water level. An obliquely incident, regular, small amplitude wave train of half height A and angular frequency ω propagates towards the breakwater with an angle θ with respect to the x axis in water of constant depth h , as shown in Fig. 1.

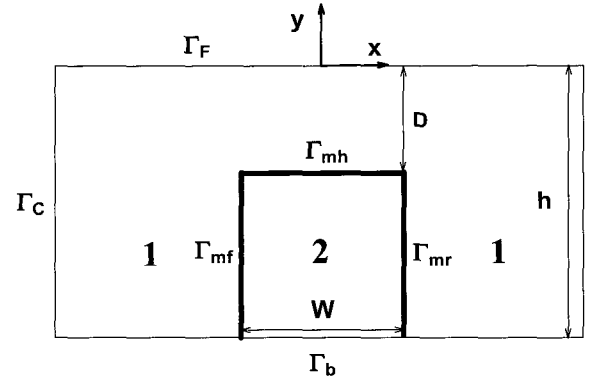


Fig. 1 Definition sketch and integration domains for Rahmen type porous membrane breakwater.

If the fluid is assumed incompressible, inviscid, and the flow irrotational, then the fluid motion can be described by velocity potential Φ that satisfies the Helmholtz equation $\nabla^2 \phi_l - k_z^2 \phi_l = 0$ within the fluid regions (Ω_l , $l=1,2$). In addition, the wave amplitude is assumed to be sufficiently small enough for linear wave theory to apply. Consequently, Φ is subject to the usual boundary conditions, linearized free surface (Γ_F), bottom (Γ_b), and approximated far field conditions (Γ_C): (see, for example, Sarpkaya and Issacson, 1981). Thus Φ may be expressed in the following form:

$$\Phi(x, y, z, t) = \text{Re}[\{\phi_o(x, y) + \phi_l(x, y)\}e^{ik_z z - i\omega t}] \quad (1)$$

where ϕ_o is the well-known incident potential, and can be written as;

$$\phi_o = \frac{igA}{\omega} \frac{\cosh k_o(y+h)}{\cosh k_o h} e^{ik_o \cos \theta x} \quad (2)$$

Also, $\text{Re}[\]$ denotes the real part of a complex expression, $i = \sqrt{-1}$, t denotes time, and $k_z = k_o \sin \theta$ is the wave number component in the z direction. The wave number of the incident wave k_o is the positive real solution of the dispersion equation $\omega^2 = k_o g \tanh k_o h$ with g being the gravitational constant. And ϕ_l is time-independent unknown scattered potentials in two fluid domains (see Fig. 1), and includes both effects of diffraction and radiation.

2.2 Permeable Membrane Boundary Condition

The required linearized kinematic boundary condition on the surface of the permeable, flexible structure may be developed based on the formulation of Wang and Ren (1993a). This may be expressed for vertical membranes as:

$$\frac{\partial \phi_1}{\partial x} = -\frac{\partial \phi_2}{\partial x} = -i\omega \xi + u(y) \quad (3)$$

where $u(y)$ is the spatial component of the normal velocity $U(y, t)$ of the fluid flow passing through a thin porous media, which is assumed to obey Darcy's law. The harmonic membrane motion is $Re[\xi e^{-i\omega t}]$. The porous flow velocity from fluid region 1 to region 2, $U(y, t) = Re[u(y) e^{-i\omega t}]$ linearly relates the pressure difference across the thin porous membrane. Therefore, it follows that

$$U(y, t) = \frac{B}{\mu} (p_1 - p_2) = \frac{B}{\mu} \rho i \omega (\phi_1 - \phi_2) e^{-i\omega t} \quad (4)$$

where B is the constant called permeability, having dimensions of a length, μ is constant coefficient of dynamic viscosity, and ρ is constant fluid density. From Eqs. (3) and (4), $u(y)$ has an expression as follows:

$$u(y) = \frac{B}{\mu} \rho i \omega (\phi_1 - \phi_2) \quad (5)$$

In order to match the two solutions on the surface of permeable membranes, ϕ and ξ , the scattered potentials must also satisfy the following linearized dynamic boundary conditions on the membrane surface:

$$\frac{d^2 \xi}{dy^2} + \lambda^2 \xi = \frac{\rho i \omega}{T} (\phi_1 - \phi_2) \quad (\text{on } \Gamma_m) \quad (6)$$

where $\lambda = \omega/c$, and c is membrane wave speed given by $\sqrt{T/m}$ with T and m being the membrane tension and mass per unit length, respectively.

2.3 Boundary Integral Equation

The fundamental solution (Green function) of the Helmholtz equation and its normal derivative of G are given, using the modified zero $K_0(\lambda r)$ and first order $K_1(\lambda r)$ Bessel function of the second kind (see, for example, Rahman and Chen, 1993), and where r is the distance from the source point to the field point. After imposing the boundary conditions, the integral equations in fluid domain can be written as

$$\begin{aligned} C\phi_1 + \int_{\Gamma_m} [k_z K_1(k_z r) \frac{\partial r}{\partial n} - \nu K_0(k_z r)] \phi_1 d\Gamma \\ + \int_{\Gamma_c} [k_z K_1(k_z r) \frac{\partial r}{\partial n} - ik_x K_0(k_z r)] \phi_1 d\Gamma \\ + \int_{\Gamma_w} [\phi_1 k_z K_1(k_z r) \frac{\partial r}{\partial n} + \frac{B}{\mu} i \rho \omega K_0(k_z r) (\phi_2 - \phi_1) \\ + sl_{\beta r} i \omega \xi K_0(k_z r)] d\Gamma + \int_{\Gamma_b} \phi_1 k_z K_1(k_z r) \frac{\partial r}{\partial n} d\Gamma \\ = - \int_{\Gamma_w} K_0(k_z r) (\frac{\partial \phi_0}{\partial n} + i \rho \omega \frac{B}{\mu} \phi_0) d\Gamma \quad (\text{in } \Omega_1) \end{aligned} \quad (7)$$

$$\begin{aligned} C\phi_2 + \int_{\Gamma_m} [\phi_2 k_z K_1(k_z r) \frac{\partial r}{\partial n} + \frac{B}{\mu} i \rho \omega K_0(k_z r) (\phi_1 - \phi_2) \\ - sl_{\beta r} i \omega \xi K_0(k_z r)] d\Gamma + \int_{\Gamma_b} \phi_2 k_z K_1(k_z r) \frac{\partial r}{\partial n} d\Gamma \\ = - \int_{\Gamma_w} K_0(k_z r) i \rho \omega \frac{B}{\mu} \phi_0 d\Gamma \quad (\text{in } \Omega_2) \end{aligned} \quad (8)$$

where C is solid-angle constant, and $\nu = \omega^2/g$ is the infinite-depth dimensionless wave number, $sl_{\beta r} = -, +, +, +$, $sl_{\beta r} = +, -, -$ for front vertical, horizontal, rear vertical membrane respectively.

The integral equations (7~8) can then be transformed into the corresponding algebraic matrix. The entire boundary is discretized into a large finite number of segments, and can be replaced by $N \times N$ matrix equations. Then, N includes numbers of segments along all boundaries, and there exist N unknowns for $\phi_1, \phi_2, N_{mf}, N_{mh}, N_{mr}$ for membrane motions, which can be given in discrete form for each segment (see, for example, Kim and Kee, 1996).

3. Numerical Results and Discussions

A boundary integral equation method, based on the distribution of simple sources along the entire boundary is developed for the numerical solution. The two vertical truncation boundaries are located sufficiently far from the membrane, such that a far field boundary condition is valid, i.e. to ensure that local wave effect is negligible.

Considering the phase velocity of incident wave (ω/k_x) and a measure of porosity with length dimension (B), the defined dimensionless porosity ($2\pi\rho\omega B/k_x\mu$) by Cho and Kim (2000) can be regarded as a sort of Reynolds number, representing the effects of both viscosity and porosity.

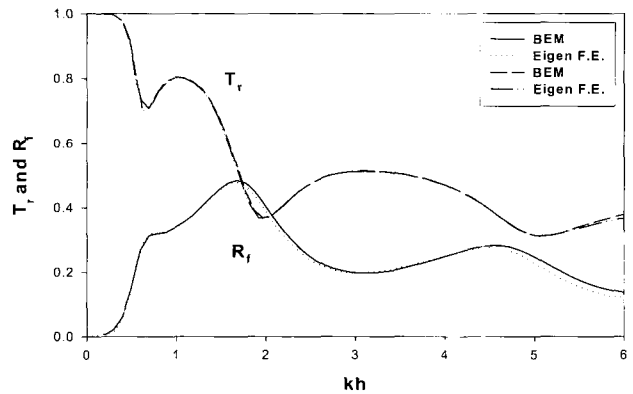


Fig. 2 Comparison of numerical method with analytic solutions. The results are for $D/h = 0.2, W/h = 1.0, \theta = 0^\circ, T_h = 0.1, 2\pi\rho\omega B/k_x\mu = 2.0$

The numerical results were checked against the energy conservation formula i.e. $R_f^2 + T_r^2 = 1$, since the energy relation is satisfied in the case of zero porosity (or an impermeable membrane). For further verification, a submerged horizontal membrane case is considered. For this horizontal system, an analytic solution has been developed for monochromatic incident waves by Cho and Kim (2000), the results of which correspond with these numerical results, as shown in Fig. 2. For two vertical non-porous membrane systems, without horizontal membrane, the comparison of numerical results and analytical solution had been checked in the previous study (Cho et al., 1998).

Transmission and reflection coefficient as a function of kh for the various permeability parameters $B=0, 1E-09, 5E-09, 1E-08, 5E-08, 1E-07, 5E-07, 1E-06$ for a beam sea ($\theta=0^\circ$) and dimensionless pre-tensions of membrane (\bar{T}) are shown in Figs. 3 & 4. The externally provided tension of the membrane is normalized by ρgh^2 , i.e. $\bar{T} = T/\rho gh^2$. The symbols $\bar{T}_f, \bar{T}_h, \bar{T}_r$ represent the non-dimensional pre-tensions for a front vertical, a horizontal, and a rear vertical membrane, respectively. The reflected and transmitted wave is gradually decreased, as permeability parameter B increases.

However, the transmitted wave for permeability coefficients higher than $1E-07$ is increased over the entire incident wave frequencies. Similar phenomena occur in the energy relation shown in Fig. 5. The error of energy relation is decreased for the permeability higher than $1E-07$. Thus, it is of particular interest to note that the best wave energy dissipation in harmonics, with hydrodynamics of membranes occurs for a system that has the permeability coefficient $1E-07$ on the membrane surfaces. For a higher permeability over the $B=1E-07$, improperly large transmitted waves surpass the wave blocking efficiency by the hydrodynamic effects of the flexible system. This could be a validation for the assumption, by Kim et al. (2000), that the permeability is not too high (say less than $B=1E-07 \text{ m}^2$) to solve the wave interaction with arbitrary porous and rigid boundaries, based on potential theory and Darcy's law. Thus, the permeability $B=1E-07$ can be defined as an effective porosity that causes maximum energy dissipation on the system as shown in Fig. 5.

The performance of the Rahmen-type wave barrier should depend on various design parameters, such as membrane parameters, submergence depth, width, incident wave angle, and frequency. First, the performance of the Rahmen-type wave barriers for various submergence depths,

after imposing the same permeability $B=1E-07$ on two vertical and one horizontal membranes, is shown in Fig. 6a-6c for various wave headings and dimensionless frequencies. The dimensionless pre-tensions of front, horizontal, and rear membranes are assumed to be given externally as $\bar{T}_{f,h,r}=0.05$.

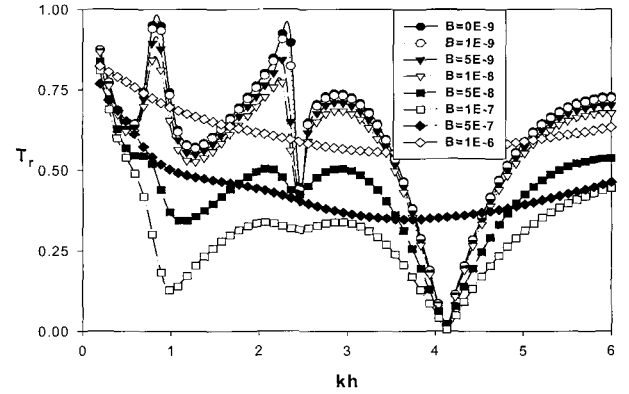


Fig. 3 Transmission Coefficient for $D/h=0.2, W/h=1.0, \theta=0^\circ$ and $\bar{T}_f=0.1, \bar{T}_h=0.05, \bar{T}_r=0.1$

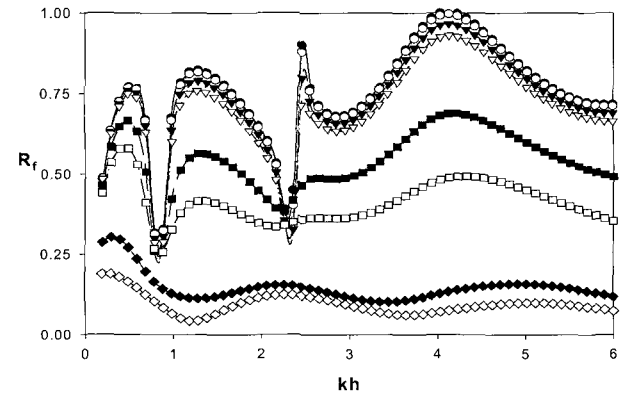


Fig. 4 Reflection Coefficient for $D/h=0.2, W/h=1.0, \theta=0^\circ$ and $\bar{T}_f=0.1, \bar{T}_h=0.05, \bar{T}_r=0.1$

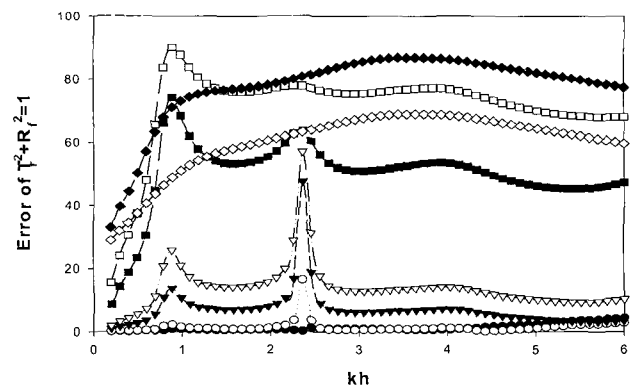
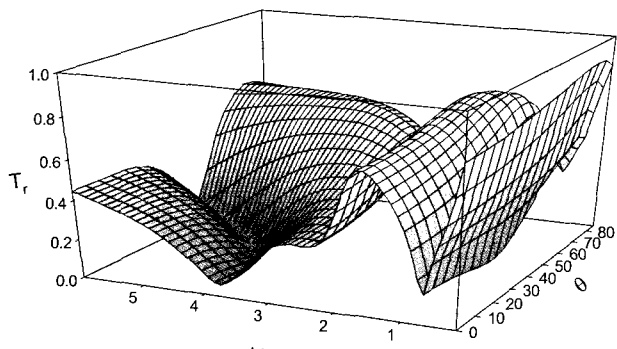
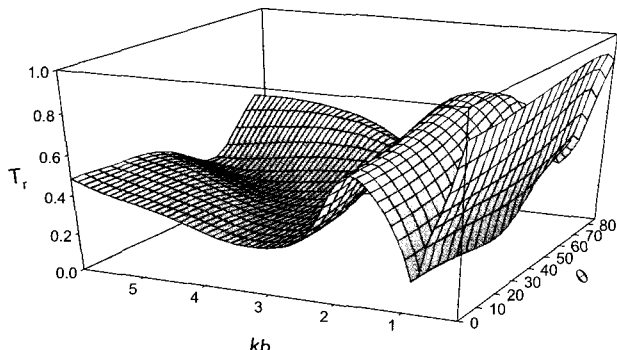


Fig. 5 Energy relation error for $D/h=0.2, W/h=1.0, \theta=0^\circ$ and $\bar{T}_f=0.1, \bar{T}_h=0.05, \bar{T}_r=0.1$

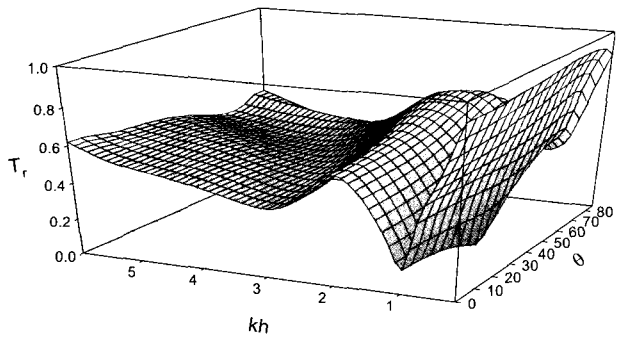
In Fig. 6a, the case of $D/h=0.2$ shows the lowest transmission in the region of $2.0 \leq kh \leq 5.5$ and $0^\circ \leq \theta \leq 55^\circ$. As the submergence depth ratio is increased to $D/h=0.25$ (Fig. 6b) and $D/h=0.3$ (Fig. 6c), the performance become worse in the region of $2.0 \leq kh \leq 5.5$ and $0^\circ \leq \theta \leq 55^\circ$ due to less wave breaking efficiency by the reduced height of vertical membranes occupying the water column. However, the performance is not sensitive to the change in the submergence depth in the long-wave regime.



(a) $D/h=0.2$



(b) $D/h=0.25$

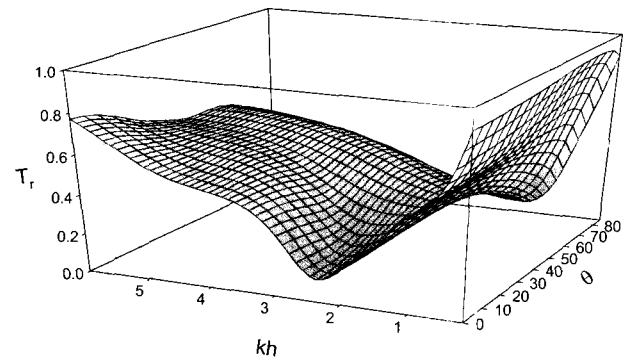


(c) $D/h=0.3$

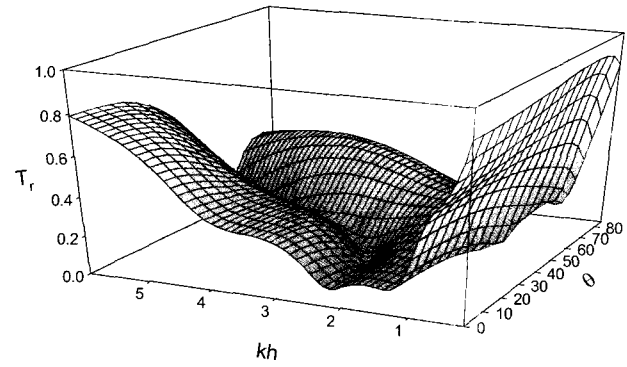
Fig. 6 Transmission coefficients for $W/h=1.0$, $\tilde{T}_{f,h,r} = 0.05$, $B=1E-07$

Figs. 7a~7c show transmission coefficients against a dimensionless wave number for various system widths with pre-tensions of flexible membranes $\tilde{T}_{f,h,r} = 0.05, 0.1, 0.15$. The larger size system is expected to allow less transmission in the wide range of frequencies and headings.

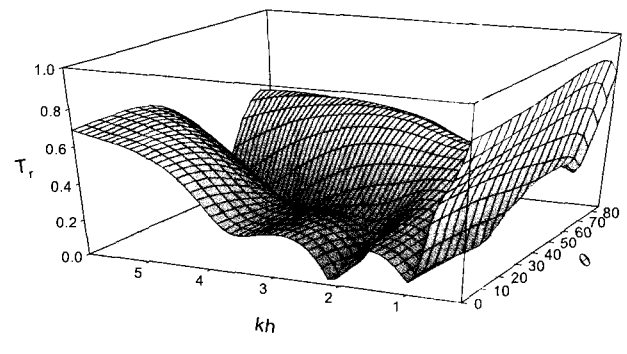
However, the performance of the system with $W/h=1.0$ is better than that of $W/h=1.25$, except in the narrow range of high frequencies and low headings. This example typically shows that a larger size system does not ensnare better performance. Highly flexible



(a) $W/h=0.75$



(b) $W/h=1.0$



(c) $W/h=1.25$

Fig. 7 Transmission coefficients for $D/h=0.25$, $\tilde{T}_{f,h,r} = 0.05, 0.1, 0.15$ and $B=1E-07$

horizontal membranes allow a large fluctuating motion that generates radiated waves for mutual cancellations against the incident waves, and has better wave blocking performance at a given submergence depth.

Figs. 8a-8b show transmission coefficients against a dimensionless wave number for various width sizes of the system with pre-tensions of flexible membranes $\bar{T}_{f,h,r} = 0.1, 0.05, 0.1$. In Fig. 8a, the system with permeability $B=0$ shows good performance in the half-arch range of frequencies along $kh \geq 2.8$ and $0 \leq \theta \leq 75^\circ$. It is interesting to note that the frequency region ensuring good performance is migrated to a higher frequency as the wave heading is increased, which is due to shorter wavelength for the high angle of attack by oblique incident waves. In the region of low frequencies, almost complete transmissions occurred, which is due, primarily, to the large fluctuating motion of membranes that generate waves in the lee side, instead of mutual cancellation against the incident waves. After imposing the permeability $B=1E-7$ on the membranes, the performance of the system is dramatically improved in the wide range of frequencies and wave headings $0^\circ \leq \theta \leq 75^\circ$ in Fig. 8b.

In Figs. 9, the distribution trend of dimensionless hydrodynamic forces on front and rear membranes is closely matched to the shapes of transmission coefficients in Fig. 8a.

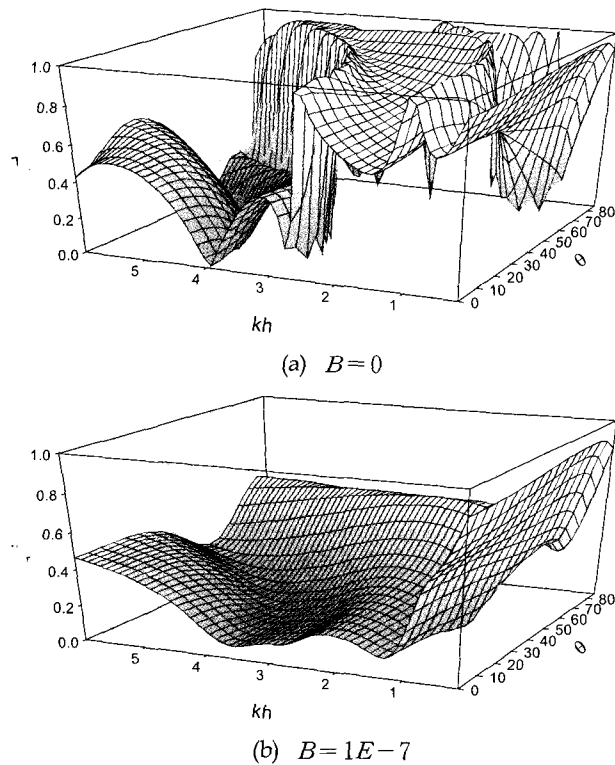


Fig. 8 Transmission coefficients for $W/h=1.0, D/h=0.25, \bar{T}_{f,h,r}=0.1, 0.05, 0.1$ and $B=1E-7$

The effects of membrane porosity on the wave-blocking performance are vividly manifested in Fig. 8b.

In the case of a porous membrane, there is wave energy dissipation through pore pores, due to fluid viscosity. Thus, the wave transmission over the effective porous membranes is significantly smaller, compared to the impermeable case, due to viscous dissipation. The generally similar trend for $\theta=0^\circ$ occurred in the motions amplitudes of impermeable and porous membranes, as shown in Fig. 10-11.

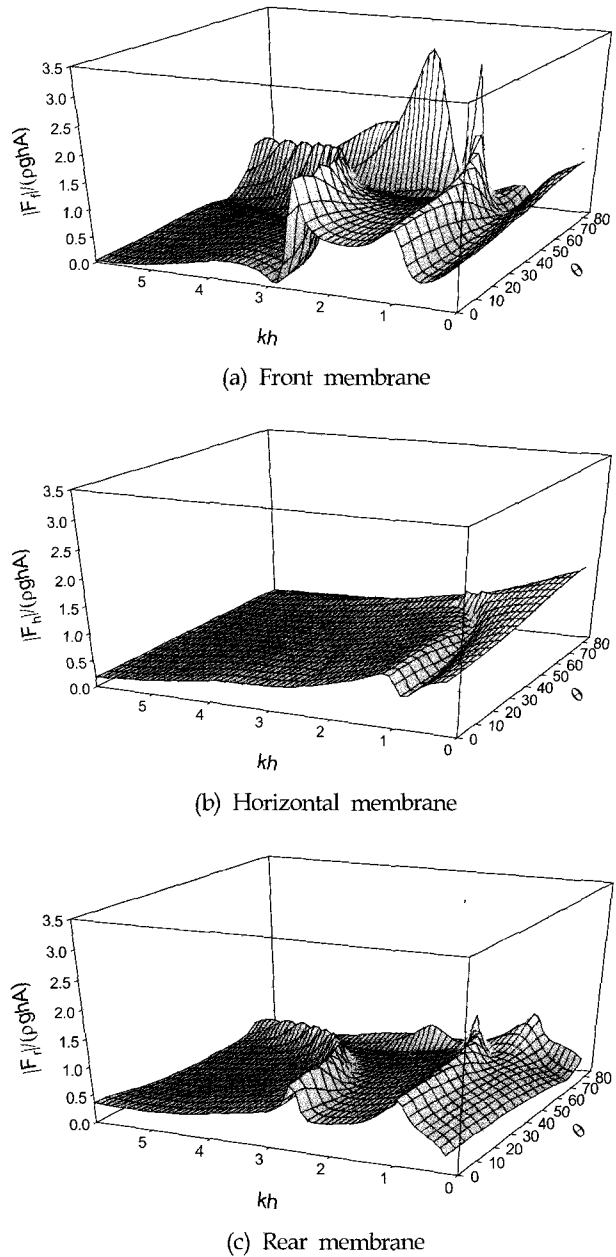
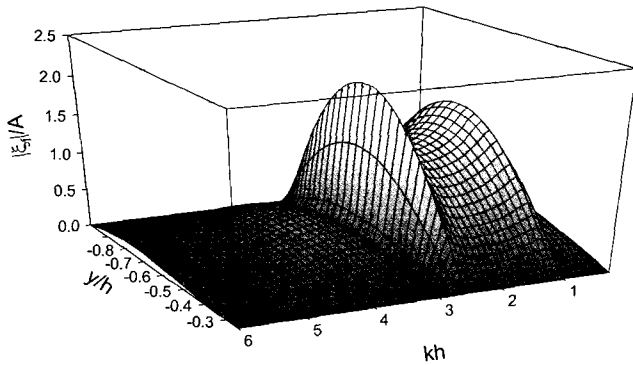


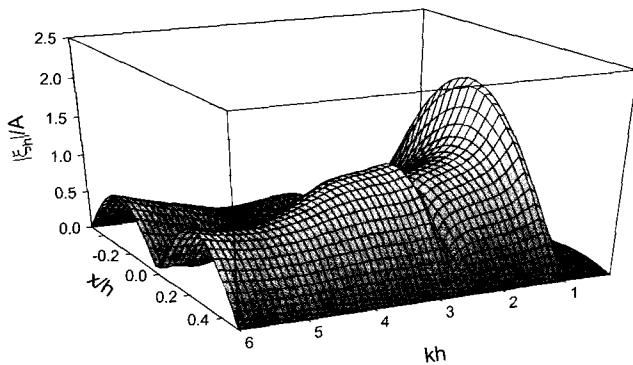
Fig. 9 Dimensionless force distribution on membranes as function of kh and θ for $\bar{T}_{f,h,r}=0.1, 0.05, 0.1, W/h=1.0, D/h=0.25, B=0$

The large motions of membranes at the frequencies $kh=1.2$ and $kh=2.8$ relates to the poor performances as wave barriers in Fig. 8a. In the motions of horizontal membranes that do not directly block incoming waves, higher modes begin to appear as the wavelength becomes shorter.

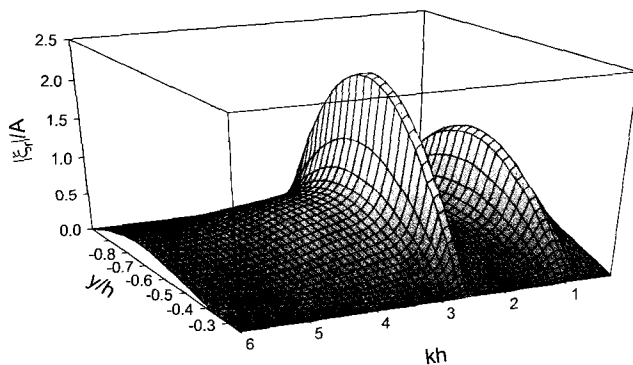
This phenomenon at the shorter wavelength region seems to be related to the high efficiency, as the wave barrier,



(a) Front membrane



(b) Horizontal membrane



(c) Rear membrane

Fig. 10 Response of membrane as function of kh and y/h for $\theta=0^\circ$, $\bar{T}_{f,h,r}=0.1, 0.05, 0.1$, $W/h=1.0$, $D/h=0.25$, $B=0$

due to favorable phase cancellation and smaller motion-induced waves, in the lee side, as shown in Fig 8a.

When the permeability is introduced on the membranes, for example, the maximum response amplitudes for rear membranes are significantly reduced, as shown in Fig. 11. This wave energy dissipation through the pores seems to be directly related to excellent wave-blocking efficiency.

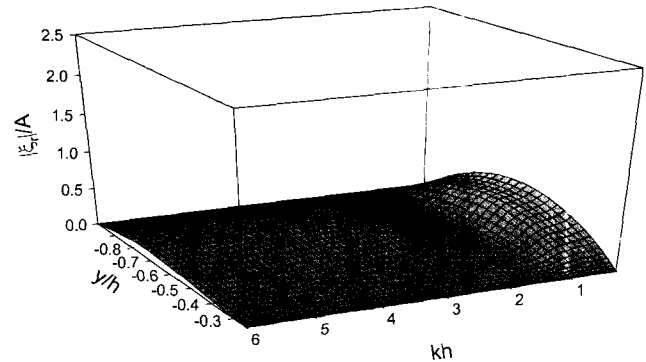


Fig. 11 Response of a rear membrane as function of kh and y/h for $\theta=0^\circ$, $\bar{T}_{f,h,r}=0.1, 0.05, 0.1$, $W/h=1.0$, $D/h=0.25$, $B=1E-07$

The effects of membrane porosity can be either positive or negative, depending on the given wave condition and system design parameters. Thus, at a certain frequency, for example around $kh=4.0$ in Fig 8a-8b, the efficiency can worsen by using porous membranes. However, the overall efficiency of a porous membrane system can be achieved along the wide frequencies and headings through the optimal combination of design parameters.

4. Summary and Conclusions

The interaction of oblique incident waves with a Rahman-type, porous, flexible membrane breakwater was investigated in the context of 2D linear hydroelastic theory. The viscous flow effects around fine pores on membranes were accounted for through the application of Darcy's law. Properly adjusted 2-D B.E.M. code has been developed for the performance analysis of a fully submerged Rahman type system. The developed program has been checked against the analytic solution for limited cases, and is in good agreement. Using the developed program, the performance was investigated for the various submergence depths, widths of the horizontal membrane, pre-tensions, permeability, and wave conditions. Based on the results analysis, it is found that the optimal system, with an effective permeability coefficient, can significantly improved the overall performances of the wave barrier along the wide range of incident waves frequencies and headings.

Acknowledgment

This research was sponsored by the Korea Research Foundation (KRF), Grant Number E00599.

References

- Choo, I.H., Kee, S.T. and Kim, M.H. (1998). "The Performance of Dual Flexible Membrane Wave Barrier in Oblique Sea" *ASCE J. of Waterways, Port, Coastal & Ocean Engineering*, Vol 124, No 1, pp 21-30.
- Choo, I.H. and Kim, M.H. (2000). "Interactions of Horizontal Porous Flexible Membrane with Waves." *ASCE J. of Waterway, Port, Coastal & Ocean Engineering*, Vol 126, No 5, pp 245-253.
- Edmond, Y.M. (1998). "Flexible Dual Membrane Wave Barrier" *ASCE J. of Waterway, Port, Coastal & Ocean Engineering*, Vol 124, No 5, pp 264-271.
- Kim, M.H. and Kee, S.T. (1996). "Flexible Membrane Wave Barrier. Part 1. Analytic and Numerical Solutions" *ASCE J. of Waterways, Port, Coastal & Ocean Engineering*, Vol 122, No 1, pp 46-53.
- Kim, M.H., Koo, W.C. and Hong, S.Y. (2000). "Wave Interactions with 2D Structures On/Inside Porous Seabed by a Two-domain Boundary Element Method" *Journal of Applied Ocean Research*, Vol 22, pp 255-266.
- Rahman, M. and Chen., M. (1993). "Boundary Element Method for Diffraction of Oblique Waves by an Infinite Cylinder." *Engineering Analysis with Boundary Elements*, Vol 11, pp 17-24.
- Sarpkaya, T. and Isaacson, M. (1981). *Mechanics of Wave Forces on Offshore Structures*, Van Nostrand Reinhold, New York.
- Wang, K.H. and Ren, X. (1993a). "An Effective Wave-Trapping System," *Ocean Engineering*, Vol 21, pp 155-178.
- Wang, K.H. and Ren, X. (1993b). "Wave Motion Through Porous Structures." *J. Engineering. Mech., ASCE*, Vol 120, No 5, pp 989-1008.
- Yu, X and Chawang, A.T. (1994). "Water Waves Above a Submerged Porous Plate." *J. Engrg. Mech., ASCE*, Vol 120, No 5, pp 1270-1278.